Food & Function

ROYAL SOCIETY OF CHEMISTRY

PAPER

View Article Online
View Journal

Cite this: DOI: 10.1039/d6fo00601a

Barley extrudates modulate the gut microbiome–metabolome axis *in vitro* through β-glucan fermentation and polyphenol biotransformation

Mariona Martínez-Subirá, [a] María Engracia Cortijo Alfonso, [a] Iván Friero, [a] Alba Macià, [a] Ramona N. Pena, [b] Natalia Molinero, [c] M. Victoria Moreno-Arribas, [c] Laura Rubió-Piqué *[a] and Marian Moralejo [a]

Barley is rich in fermentable dietary fiber and phenolic compounds, both of which have recognized benefits for gut health and whose functionality is influenced by processing. Here, four barley genotypes differing in β-glucan content, type of starch, and phenolic profiles were extruded to obtain ready-to-eat products, which were then evaluated using a combined *in vitro* digestion–colonic fermentation model. The gastrointestinal fate of β-glucans and phenolics, short-chain fatty acids production, phenolic metabolite formation, and gut microbiota composition were assessed. After digestion, substantial amounts of β-glucans and phenolics remained in the non-bioaccessible fraction, supporting their relevance as substrates for colonic fermentation. During fermentation, the β-glucan-rich genotypes Annapurna® and Hilose® showed the strongest butyrogenic response, while the purple-grain genotype DHL-151340, characterized by a flavone- and anthocyanin-rich profile, showed an earlier and more pronounced accumulation of low-molecular-weight phenolic catabolites. Compared with the control, barley extrudates induced time-dependent shifts in microbiota composition, although community profiles tended to converge at later fermentation stages. Overall, genotype- and processing-driven differences translated into distinct fermentation and phenolic biotransformation footprints, highlighting the relevance of barley matrix composition in shaping the colonic fate of cereal bioactive compounds.

Received 6th February 2026,
Accepted 30th April 2026

DOI: 10.1039/d6fo00601a

rsc.li/food-function

1. Introduction

Barley (*Hordeum vulgare* L.) has gained increasing attention as an ingredient for the development of cereal-based foods with added nutritional value. Compared with other commonly consumed cereals, barley is particularly rich in bioactive compounds, especially soluble dietary fiber such as β-glucans and a wide range of phenolic compounds, mainly phenolic acids and flavonoids.[1–4] The intake of barley-derived products has been associated with beneficial effects on lipid and glycemic metabolism, immune response, and gut microbiota modulation, largely attributed to these components.[5–7]

However, the physiological effects of barley depend not only on its chemical composition, but also on the food matrix and the processing conditions applied before consumption.[8] In this context, extrusion cooking is widely used in the production of ready-to-eat cereal products, but it also induces important chemical and structural transformations that may alter the solubility, extractability, and molecular characteristics of β-glucans and phenolic compounds.[9–11] These matrix modifications are expected to influence the gastrointestinal release of bioactive compounds and their subsequent availability for microbial fermentation in the colon.[12]

Both β-glucans and phenolic compounds are particularly relevant in this regard. β-Glucans are not digested by human enzymes and therefore reach the large intestine, where they are fermented by the intestinal microbiota, leading to the production of short-chain fatty acids (SCFAs) which are key mediators of gut and metabolic health.[13–15] Likewise, a substantial proportion of cereal phenolics exhibit limited bioaccessibility in the upper gastrointestinal tract and reaches the colon, where it undergoes extensive microbial biotransformation.[14,16,17] In turn, these compounds and their derived metabolites can also shape microbial composition and activity, highlighting the bidirectional relationship between cereal bioactives and the gut ecosystem.[18–22]

Despite growing evidence on the health-related potential of barley, most studies have focused on raw grains, isolated frac-

[a]*University of Lleida–Agrotecnio CERCA Center, Av. Alcalde Rovira Roure 191, 25198 Lleida, Spain. E-mail: laura.rubio@udl.cat*
[b]*Department of Animal Science, University of Lleida–Agrotecnio CERCA Center, Av. Alcalde Rovira Roure 191, 25198 Lleida, Spain*
[c]*Institute of Food Science Research (CIAL), CSIC-UAM, 28049 Madrid, Spain*

tions, or specific classes of compounds, whereas barley is typically consumed as a processed food matrix.[13,17,21,22] Moreover, previous studies have generally addressed digestion, fermentation, or compositional changes separately, rather than integrating the gastrointestinal and colonic fate of multiple bioactive components. In this regard, our previous studies have contributed to understanding both the digestive fate of cereal phenolics and the impact of extrusion on the nutritional and phenolic profile of barley-based extrudates.[11,14] However, the downstream consequences of these matrix- and processing-induced differences on gastrointestinal bioaccessibility, microbial metabolism, and gut microbiota activity remain largely unexplored.

Therefore, the aim of this study was to investigate the gastrointestinal fate of β-glucans and phenolic compounds from extruded barley-based products obtained from contrasting genotypes, and to assess how these compositional differences translate into microbial fermentation patterns and metabolite production. For this purpose, extruded barley-based products were subjected to *in vitro* gastrointestinal digestion followed by human fecal batch fermentation, and their effects on SCFAs production, phenolic metabolism, and gut microbiota composition were comprehensively assessed.

2. Materials and methods

2.1. Chemicals and reagents

The digestive enzymes and secretions used (α-amylase, pepsin, pancreatin, and bile salts) were purchased from Sigma-Aldrich (St Louis, MO, USA), all of porcine origin. SCFAs standards such as acetic ($C_2H_4O_2$), propionic ($C_3H_6O_2$), isobutyric ($C_4H_8O_2$), butyric ($C_4H_8O_2$), isovaleric ($C_5H_{10}O_2$), valeric ($C_5H_{10}O_2$), hexanoic ($C_6H_{12}O_2$), and 4-methylvaleric ($C_6H_{12}O_2$) acids were purchased from Sigma-Aldrich (St Louis, MO, USA). Phenolic compound standards such as cyanidin-3-*O*-glucoside chloride, luteolin-7-*O*-glucoside, methyl luteolin (chrysoeriol), and luteolin-7-*O*-glucuronide were purchased from Extrasynthese (Genay, France), 4-hydroxybenzoic acid, 3,5-dimethoxy-4-hydroxybenzoic acid (aka syringic acid), 3,5-dimethoxy-4-hydroxycinnamic acid (aka sinapic acid), and catechin were purchased from Sigma-Aldrich (St Louis, MO, USA); 4′-hydroxy-3′-methoxycinnamic acid (aka ferulic acid) was obtained from Fluka (Buchs, Switzerland). Methanol (HPLC grade), acetonitrile (HPLC grade), acetic acid, formic acid, and hydrochloric acid (HCl) were purchased from Scharlab Chemie (Sentmenat, Catalonia, Spain). Sodium hydroxide (NaOH) was obtained from Fluka (Buchs, Switzerland). Water of Milli-Q quality was supplied by Millipore Corp. (Bedford, MA, USA). Stock solutions of standard compounds were prepared by dissolving each standard compound in methanol at a concentration of 1000 mg L^{-1}, and stored in a dark flask at −30 °C. The nomenclature of the phenolic catabolites used in this paper is based on the recommendations made by Kay *et al.* and, more recently, by Curti *et al.*[23,24]

2.2. Raw material

Four hull-less barley genotypes with contrasting compositional characteristics and suitability for food applications were selected for this study:

- Annapurna®: low-amylose starch, high β-glucan content, yellow grains
- DHL-151340: normal-amylose starch, medium β-glucan content, purple grains
- Hilose®: high-amylose starch, high β-glucan content, yellow grains.
- SBExpCE: normal-amylose starch, medium β-glucan content, yellow grains

Barley grains were supplied by Semillas Batlle SA (Bell-Lloc d'Urgell, Lleida, Spain). For the extrusion process, the grains were milled to 1 mm using a Brabender mill equipped with a 1 mm screen (Brabender® GmbH & Co., Duisburg, Germany). For chemical analyses, samples were milled to 0.5 mm using a Foss Cyclotec 1093™ mill equipped with a 0.5 mm screen (FOSS, Barcelona, Spain).

2.3. Extrusion process

The extrusion process was carried out using a co-rotating twin-screw extruder (TwinLab-F 20/40, C.W. Brabender® GmbH & Co. KG, Duisburg, Germany) equipped with a 2 mm die. To obtain ready-to-eat barley-based products, the extrusion conditions were individually adjusted for each genotype based on their compositional characteristics, thereby ensuring appropriate structural and nutritional properties. Accordingly, the process parameters were applied as operational ranges, including a screw speed of 360–500 rpm, a feed rate of 3.5–3.8 kg h^{-1}, and a moisture content between 12% and 17%. The temperature profile was also adapted across the six heating zones (Z1: 53–70 °C, Z2: 94–110 °C, Z3: 100–163 °C, Z4: 130–174 °C, Z5: 143–197 °C, Z6: 143–197 °C) to provide the thermal and mechanical energy required for adequate expansion and structural development. After extrusion, the products were milled using a Foss Cyclotec 1093™ mill with a 0.5 mm screen to obtain a uniform particle size for subsequent analyses.

2.4. *In vitro* gastrointestinal digestion of barley extrudates

In vitro gastrointestinal digestions of barley extrudates were performed following the standardized INFOGEST protocol,[25] simulating oral, gastric, and small intestinal phases. A 5 g portion of each extruded barley sample was used as an analytically manageable test portion while maintaining the recommended food-to-fluid ratios and enzyme activities. Digestion resulted in a final volume of approximately 74 mL, yielding a food-to-fluid ratio (0.07 g mL^{-1}), within the physiological range expected for cereal consumption (0.06–0.24 g mL^{-1}), based on typical serving sizes (30–60 g) and postprandial gastric volumes (250–500 mL).

Briefly, extrudate samples were mixed with simulated salivary fluid (pH 7, 75 U mL^{-1} α-amylase) and incubated for 2 min at 37 °C during the oral phase. For the gastric phase, simulated gastric fluid containing porcine pepsin (2000 U

mL^{-1}) was added, the pH was adjusted to 3 with HCl and the samples were incubated at 37 °C for 2 h under orbital agitation (200 rpm). Subsequently, simulated intestinal fluid (pH 7, 10 mmol L^{-1} porcine bile salts, and 100 U mL^{-1} pancreatin) was added, and the samples were incubated at 37 °C for 2 h. After digestion, samples were centrifuged at 13 000*g* for 10 min at 4 °C to separate the bioaccessible fraction (supernatant) from the non-bioaccessible fraction (residue) for colonic fermentation. Both fractions were lyophilized and stored at −80 °C for further analyses. Target compounds (β-glucans, starch, and phenolic compounds) were quantified on a dry weight basis. To account for differences in mass recovery, results were corrected by the dry weight of each fraction and normalized to the dry weight of the initial extruded sample.

2.5. Fecal sample collection and storage

Fecal samples were collected from six healthy adult volunteers (three men and three women, 28–40 years old, BMI 18.5–24.9 kg m^{-2}) with no gastrointestinal disorders and no use of antibiotics or prebiotics during the 4 months before collection. Samples were collected in sterile airtight containers and transported immediately to the laboratory. Anaerobic conditions during transport and handling were maintained using anaerobic jars containing AnaeroGen™ sachets (Oxoid Ltd, Basingstoke, UK). Samples were kept at 4 °C and used within 24 h.

In the laboratory, individual fecal samples were pooled to prepare a microbial inoculum, supplemented with 20% glycerol for preservation, and stored at −80 °C until use in colonic fermentations, following the methodology described by Pérez-Burillo *et al.*[26] The study was conducted in accordance with the Declaration of Helsinki and approved by the Ethics Committee of Hospital Universitari Arnau de Vilanova (Lleida, Spain) (approval code: CEIC-3250). All participants provided written informed consent.

2.6. *In vitro* colonic batch fermentations

In vitro colonic batch fermentations were performed according to Pérez-Burillo *et al.*[26] with minor modifications. For the fermentation assays, the pooled fecal inoculum was thawed, centrifuged to remove glycerol, and resuspended in 0.1 M phosphate buffer (pH 7) to obtain a 32% suspension. Each fermentation tube contained 0.5 g of the non-bioaccessible residue, 10% of the intestinal supernatant, 7.5 mL of fermentation medium (15 g L^{-1} peptone and 50 mL L^{-1} of reducing solution), and 2 mL of fecal suspension. Control incubation was performed using residues from blank digestions. Fermentations were carried out in anaerobic chambers at 37 °C with continuous orbital agitation (120 rpm). Anaerobic conditions were established using AnaeroGen™ sachets (Oxoid Ltd, Basingstoke, UK), and all manipulations were performed under a nitrogen flow to minimize oxygen exposure. All incubations were performed in triplicate in identical experimental conditions. Samples and control were collected at different time points (0, 2, 6, 10, 24, and 48 h). Fermentation samples were divided into two portions: one for microbiota analysis and another for metabolite analysis. The latter was freeze-dried, and all samples were stored at −80 °C until analysis.

2.7. β-Glucans, arabinoxylans, total starch, and amylose determinations

Total β-glucans, arabinoxylans, starch, and amylose contents were quantified using the mixed-linkage β-glucan assay (K-BGLU), D-xylose assay (K-XYLOSE), total starch assay (AA/AMG), and amylose/amylopectin assay (K-AMYL) kits from Megazyme (Megazyme International Ireland Ltd, Bray, Ireland).

2.8. Analysis of phenolic compounds and microbial phenolic metabolites

The analysis of phenolic compounds was performed according to Cortijo-Alfonso *et al.*[27] Briefly, free phenolics were extracted using an extraction solution of methanol/Milli-Q water/formic acid (79.5/19.5/1, v/v/v). The remaining solid residue was then subjected to alkaline hydrolysis to release the bound phenolic fraction. Bound phenolic extracts were cleaned using microElution solid-phase Extraction (μSPE) with OASIS HLB cartridges (2 mg) (Waters, Milford, MA, USA). The phenolic compounds were eluted from these micro-cartridges with methanol (2 × 50 μL) and directly injected into the analytical system. Phenolic compounds were quantified by ultraperformance liquid chromatography (UPLC) coupled to tandem mass spectrometry (MS/MS) (Waters, Milford, MA, USA), using chromatographic conditions as previously reported in our study.[27] Analyses were carried out on a triple quadrupole mass spectrometer equipped with an electrospray ionization (ESI) source. Quantification was performed using selected reaction monitoring (SRM), with MS parameters as previously described.[27]

2.9. Analysis of short-chain fatty acids

SCFAs were determined by gas chromatography coupled to flame ionization detector (GC-FID) according to Calderón-Pérez *et al.*[28] Briefly, 0.1 g of lyophilized colonic fermentation samples were mixed with 1 mL of acidified Milli-Q water (pH 2–3 adjusted with H_3PO_4) containing 4-methylvaleric acid as the internal standard (1.85 mg mL^{-1}). Samples were shaken for 15 min and centrifuged for 15 min at 13 000*g* at 4 °C. The supernatant resulting from the centrifugation was filtered with a 0.22 μm nylon filter (Tecnokroma, Barcelona, Spain) and passed into GC microvials containing an insert for analysis. Finally, the samples were analyzed by GC according to our previous work.[28]

2.10. Bacterial DNA extraction and 16S rRNA gene sequencing

Total bacterial DNA was isolated from colonic fermentation samples using the HigherPurity™ soil DNA isolation kit (Canvax Reagents SL, Valladolid, Spain), according to the manufacturer's instructions with minor modifications: frozen wet

samples were disrupted twice in a bead homogenizer (BeadMill 4, ThermoFisher) with two borosilicate 2 mm beads and the kit's lysis buffer, and incubated at 95 °C for 5 min. Then, sample tubes were spun at 10 000*g* for 30 s and the supernatant was transferred to a fresh tube to follow with the manufacturer's instructions. In the final step, the DNA was eluted from the column in a volume of 100 μL. DNA concentration and quality were evaluated by spectrophotometry (Nanodrop-100, ThermoFisher, Barcelona, Spain) and fluorometry with the dsDNA HS Assay kit (Qubit 4, Invitrogen, Carlsbad, CA). The V3–V4 region of the 16S rRNA gene was amplified using previously described primers[18] and sequenced with 2 × 300 bp paired-end reads using the Illumina MiSeq platform (Illumina, San Diego, CA, USA) at the Centre for Genomic Regulation (CRG), Barcelona, Spain. RStudio v.1.3.1093 software was employed to process the files with raw reads from the Illumina® instrument. Quality profiles were first assessed with FastQC, and low-quality reads ($Q < 20$) and potential contaminant sequences were removed. Forward and reverse reads were truncated at 250 bp, based on quality scores. Reads were then denoised, merged, and filtered to remove chimeras following the standard DADA2 pipeline (https://benjjneb.github.io/dada2/tutorial.html).[29] This approach allows inference of Amplicon Sequence Variants (ASVs) with single-nucleotide resolution. A total of 1797 ASVs were obtained. Taxonomic assignment was performed using the naïve Bayesian classifier implemented in DADA2 using the Silva v.138.2 reference database.[29] Alpha-diversity was estimated based on ASVs counts by calculating the observed ASVs, Shannon and Simpson indices through the "Phyloseq" package (v1.44.0). Beta-diversity was assessed *via* Bray–Curtis dissimilarity matrix and visualized using non-metric multidimensional scaling plot (NMDS). Relative abundances at each taxonomic level were calculated per individual sample.

2.11. Statistical analysis

Results are expressed as the mean of at least two or three replicates. Data from β-glucans, arabinoxylans, total starch, amylose, and phenolic compounds were analyzed by one-way ANOVA followed by Tukey's *post hoc* test ($p < 0.05$). These analyses were performed using JMP® Pro 16 (SAS Institute Inc., Cary, NC, USA).

During *in vitro* colonic fermentation, differences among extracts and fermentation times for β-glucans, SCFAs, phenolic compounds, and phenolic-derived metabolites were evaluated by two-way ANOVA, followed by Tukey's or Games–Howell *post hoc* tests, depending on variance homogeneity. Two-way ANOVA for SCFA and 16S rRNA gene-based sequencing data were performed using XLSTAT software (version 2022.4.1; Addinsoft).

Alpha-diversity metrics (observed amplicon sequence variants (ASVs), Shannon, and Simpson) were assessed using the Mann–Whitney *U* test with Benjamini–Hochberg correction for multiple comparisons. Beta-diversity differences were assessed by PERMANOVA. These analyses were conducted using R software (version 4.3.0) and RStudio (version 1.3.1093).

To reduce data heterogeneity and improve visualization in the heatmap, a square root transformation ($x' = \sqrt{(\log(x + 1))}$) was applied to the mean values. This transformation helps to normalize the data distribution, particularly when variables differ greatly in magnitude.

Associations between taxa at genus level and different metabolite profiles were evaluated through Spearman's correlation test, applying Benjamini–Hochberg multivariate analysis correction *post hoc* test (FDR = 0.05). All correlation analyses performed were conducted using qdapTools package available for R software (v. 4.3.0) and RStudio (v.1.3.1093).

3. Results and discussion

This study provides an integrated assessment of how barley genotype and extrusion-induced matrix modifications shape the gastrointestinal and colonic fate of bioactive compounds. Unlike previous studies[13,17,21,22] focused on raw grains, isolated fractions, or selected compounds, it combines *in vitro* digestion, colonic fermentation, SCFA production, phenolic biotransformation, and microbiota modulation in extruded barley matrices differing in β-glucan content, starch type, and phenolic profile.

3.1. Changes in chemical composition associated with extrusion processing

Before extrusion, the four barley genotypes showed marked differences in chemical composition and bioactive compound profiles, as shown in Table 1. Hilose® and Annapurna® presented the highest β-glucan content, reaching 11.4 and 10.0 g per 100 g, respectively, whereas DHL-151340 and SBExpCE had significantly lower amounts. Arabinoxylan content was relatively similar across genotypes. Total starch content was lower in Hilose® and Annapurna®, at approximately 45%, compared with DHL-151340 and SBExpCE, which exhibited values close to 60%. As expected, Hilose® displayed the highest amylose content, reaching 29.4%. In contrast, Annapurna® showed the lowest value at 4.5%, consistent with its waxy phenotype. As shown in Table 1, Hilose® and DHL-151340 flours exhibited the highest total phenolic contents (1345 and 1360 μmol per 100 g, respectively), with phenolic acids being the predominant class, present in both free and cell wall-bound forms (SI Table S1). The phenolic profile differed substantially between the yellow-grain genotypes and the purple-grain genotype. The purple genotype was characterized by higher levels of flavone glycosides and anthocyanins, reaching 294 μmol per 100 g and 44.4 μmol per 100 g, respectively, and by a distinctive profile dominated by methyl-luteolin and related derivatives, along with the exclusive presence of anthocyanins.[30] In contrast, yellow genotypes were richer in flavan-3-ols, with contents ranging from 103 to 249 μmol per 100 g, mainly represented by catechins and proanthocyanidins, in agreement with previous reports.[30] Irrespective of grain color, phenolic acids constituted the predominant phenolic family in all genotypes and were mainly present in the bound fraction with concentrations

Table 1 β-Glucans (g per 100 g), arabinoxylans (g per 100 g), total starch (g per 100 g), amylose (%), and phenolic compounds (μmol per 100 g) contents in flours and extruded products from different barley genotypes

Genotype	β-Glucans	Arabinoxylans	Total starch	Amylose	Total phenolic compounds	Total flavan-3-ols	Total flavones	Total anthocyanins	Total phenolic acids
Flours									
Annapurna®	10.0 ± 0.3 b A	6.1 ± 0.2 b A	44.8 ± 0.8 b B	4.5 ± 0.3 c B	1034.0 ± 61.8 b A	235.1 ± 14.1 a A	2.9 ± 0.2 b A	n.d.	796.1 ± 47.9 b A
Hilose®	11.4 ± 0.4 a A	7.1 ± 0.2 a A	44.5 ± 0.9 b B	29.4 ± 0.1 a B	1344.6 ± 16.5 a A	249.0 ± 0.2 a A	9.5 ± 0.4 b A	n.d.	1086.1 ± 16.7 a A
DHL-151340	5.6 ± 0.1 c A	6.6 ± 0.1 ab A	59.5 ± 1.4 a A	20.9 ± 1.8 b B	1359.5 ± 31.8 a A	71.5 ± 4.1 c A	294.1 ± 6.0 a A	44.4 ± 3.8 A	949.5 ± 45.8 ab A
SBExpCE	4.6 ± 0.2 c A	5.2 ± 0.2 c A	61.3 ± 2.7 a A	20.3 ± 0.3 b B	1013.4 ± 60.5 b A	102.9 ± 1.6 b A	6.9 ± 0.4 b A	n.d.	903.6 ± 58.5 ab A
Extrudates									
Annapurna®	7.0 ± 0.2 a B	5.9 ± 0.3 a A	57.6 ± 1.4 ab A	11.6 ± 1.4 d A	801.5 ± 37.2 b B	68.4 ± 3.8 a B	1.7 ± 0.0 b B	n.d.	731.5 ± 41.1 a A
Hilose®	6.8 ± 0.1 a B	6.5 ± 0.3 a A	53.7 ± 1.4 b A	44.8 ± 2.2 a A	881.1 ± 7.8 b B	75.7 ± 3.1 a B	4.9 ± 0.6 b B	n.d.	800.4 ± 5.4 a B
DHL-151340	4.9 ± 0.1 b B	5.8 ± 0.4 a B	58.5 ± 2.0 ab A	33.9 ± 0.2 b A	1174.2 ± 15.4 a B	36.1 ± 1.0 b B	297.5 ± 11.1 a A	22.8 ± 2.5 B	817.8 ± 0.8 a A
SBExpCE	4.5 ± 0.1 b A	4.5 ± 0.1 b B	60.4 ± 0.6 a A	28.9 ± 1.1 c A	838.8 ± 21.4 b A	42.7 ± 3.7 b B	2.3 ± 0.0 b B	n.d.	793.9 ± 25.2 a A

Results are expressed as means. Lowercase letters indicate significant differences among genotypes within the same matrix (flour or extruded (one-way ANOVA), whereas uppercase letters indicate significant differences between flour and extruded samples within the same genotype (two-way ANOVA) followed by the Tukey–Kramer HSD *post hoc* test ($p < 0.05$). n.d., not detected.

ranging from 783 to 1078 μmol per 100 g. This fraction was dominated by 4′-hydroxy-3′-methoxycinnamic acid (aka ferulic acid) and its derivatives, as shown in Table 1 and SI Table S1, which are known to be strongly associated with the cereal cell wall matrix.

Following extrusion processing, the resulting barley products showed marked differences in chemical composition across genotypes, as shown in Table 1. Compared with their respective raw flours, β-glucans content showed a moderate decrease, particularly in Hilose® and Annapurna® extrudates, declining from 11.4 to 6.8 g per 100 g and from 10.0 to 7.0 g per 100 g, respectively. This reduction is likely associated with β-glucan chain depolymerization and reduced extractability caused by interactions with the starch–protein matrix.[31] In contrast, arabinoxylans showed limited changes after extrusion, consistent with their higher resistance to thermal and mechanical stress.[32] Amylose content increased in all genotypes after extrusion processing, with the most pronounced increase observed in Annapurna® and DHL-151340 extrudates, rising from 4.5% to 11.9% and from 20.9% to 33.9%, respectively. This effect can be attributed to the greater susceptibility of amylopectin to thermal and mechanical stresses, which promotes partial depolymerization and results in a relative increase in the amylose proportion.[33]

Extrusion processing was associated with a significant reduction in total phenolic content, with an average decrease of approximately 20% across genotypes, mainly affecting flavan-3-ols and anthocyanins, as shown in Table 1 and SI Table S1. These compounds are known to be thermosensitive.[34] In contrast, the proportion of free phenolic acids increased, likely as a result of the disruption of phenolic–cell wall linkages, which may contribute to enhanced bioaccessibility.[35]

Overall, extrusion processing resulted in marked modifications in the chemical composition of genotype-specific barley products, including a moderate reduction in β-glucan content, starch reorganization associated with an increased amylose proportion, and a decrease in thermosensitive phenolic compounds. Despite these changes, extrusion-induced structural modifications may enhance the functionality and bioaccessibility of barley bioactive components in the final ready-to-eat products. These compositional differences were further explored by principal component analysis (PCA) based on the data presented in Table 1 (SI Fig. S1). The PCA revealed a clear separation of samples according to both genotype and processing, with extruded products clustering distinctly from their corresponding flours. The first principal component (PC1, 53.4%) was mainly associated with carbohydrate-related variables, particularly β-glucans and total starch, whereas the second component (PC2, 22.0%) was driven by phenolic composition. Accordingly, extruded samples such as Hilose® and Annapurna® were positioned closer to variables related to β-glucan content, whereas the purple-grain extrudate DHL-151340 was clearly separated along PC2, reflecting its distinct phenolic profile rich in flavones and anthocyanins. SBExpCE showed an intermediate distribution between these

groups. These results support the differentiation of extruded barley products, highlighting their potential classification based on prebiotic-related and antioxidant-associated components.

3.2. Influence of gastrointestinal digestion on β-glucan, type of starch, and phenolic compounds

A key question in the present study was whether the compositional differences retained after extrusion were functionally translated into distinct bioaccessible and non-bioaccessible fractions during upper gastrointestinal digestion. This distinction is particularly relevant because the bioaccessible fraction determines the compounds potentially available for absorption, whereas the non-bioaccessible fraction defines the substrates that remain available for microbial metabolism in the colon.

As shown in Table 2 and SI Table S2, β-glucans were partially solubilized during digestion, with 40–55% recovered in the bioaccessible fraction, whereas a relevant proportion remained associated with the non-bioaccessible residue.

These results indicate extensive β-glucan solubilization during digestion, likely promoted by extrusion-induced disruption of the food matrix and partial polysaccharide depolymerization.[31] Although β-glucans are not absorbed in the small intestine, their soluble fraction contributes to physiological effects, including increased intestinal viscosity and modulation of postprandial glycaemic and lipid responses.[36] These functional properties are further influenced by structural features such as molecular weight and viscosity.[37] Importantly, the predominance of β-glucans in the bioaccessible fraction reflects their release from the food matrix and solubility rather than intestinal absorption. Both bioaccessible and non-bioaccessible fractions are therefore expected to reach the colon, where they may undergo partial fermentation and contribute to SCFAs production.[13,14]

The amount of starch recovered in the non-bioaccessible fraction ranged from 6.07 to 12.49 g per 100 g, with the highest values observed in Hilose® and the lowest in Annapurna®. The higher starch levels detected in Hilose® may be associated with the elevated amylose content of the extruded product, which is known to promote the formation of digestion-resistant starch structures, particularly after extrusion processing.[38] However, the starch quantified in this fraction does not exclusively correspond to resistant starch but may also include starch that was not completely digested during the *in vitro* gastrointestinal digestion process.

The INFOGEST protocol, while widely accepted for simulating human digestion, primarily considers pancreatic α-amylase activity during the intestinal phase and does not include brush-border enzymes involved in the final hydrolysis of starch-derived oligosaccharides.[25] This methodological limitation, acknowledged within the protocol due to the lack of standardization of additional enzyme activities and exposure times,[25,39] may lead to partially digested starch in the non-bioaccessible fraction. Consequently, the fraction analyzed in this study likely consisted of a mixture of resistant

Table 2 β-Glucans (g per 100 g extrudate), total starch (g per 100 g extrudate), and phenolic compounds (μmol per 100 g extrudate) in the bioaccessible and non-bioaccessible fractions of extruded barley samples after *in vitro* gastrointestinal digestion

	Annapurna®		Hilose®		DHL-151340		SBExpCE	
	Bioaccessible fraction	Non-bioaccessible fraction	Bioaccessible fraction	Non-bioaccessible fraction	Bioaccessible fraction	Non-bioaccessible fraction	Bioaccessible fraction	Non-bioaccessible fraction
β-Glucans	2.89 ± 0.15 a	1.79 ± 0.05 c	3.03 ± 0.02 a	2.27 ± 0.06 b	2.68 ± 0.01 a	1.28 ± 0.03 d	1.80 ± 0.01 c	1.42 ± 0.07 d
Total starch	27.24 ± 0.11 b	6.07 ± 0.07 g	24.23 ± 0.12 c	12.49 ± 0.07 d	31.58 ± 0.33 a	7.92 ± 0.00 f	31.83 ± 0.22 a	10.25 ± 0.22 e
Total phenolic compounds	121.54 ± 8.75 d	686.29 ± 25.17 a	135.39 ± 3.94 d	580.94 ± 8.21 b	230.63 ± 4.82 c	660.43 ± 6.34 a	132.36 ± 0.94 d	502.39 ± 27.03 b
Total flavan-3-ols	22.26 ± 0.70 c	21.66 ± 1.98 c	38.08 ± 0.06 ab	39.97 ± 2.47 a	23.66 ± 0.60 c	11.44 ± 0.52 d	32.86 ± 0.24 b	14.21 ± 0.43 d
Total free flavones	0.74 ± 0.04 b	0.56 ± 0.04 b	1.47 ± 0.14 b	1.42 ± 0.10 b	124.55 ± 5.99 a	116.59 ± 3.63 a	0.85 ± 0.05 b	0.52 ± 0.01 b
Total bound flavones	0.01 ± 0.00 c	0.20 ± 0.01 c	0.02 ± 0.00 c	0.14 ± 0.00 c	0.75 ± 0.02 b	4.53 ± 0.12 a	0.01 ± 0.00 c	0.12 ± 0.00 c
Total anthocyanins	n.d.	n.d.	n.d.	n.d.	14.35 ± 0.80 a	3.67 ± 0.12 b	n.d.	n.d.
Total free phenolic acids	7.65 ± 0.16 b	1.48 ± 0.07 d	7.88 ± 0.46 b	2.22 ± 0.20 d	20.45 ± 0.51 a	4.16 ± 0.34 c	8.88 ± 0.00 b	2.03 ± 0.04 d
Total bound phenolic acids	90.89 ± 9.65 c	662.39 ± 23.20 a	87.94 ± 3.68 c	537.19 ± 10.99 b	46.87 ± 0.43 c	520.04 ± 1.85 b	89.75 ± 1.22 c	485.51 ± 27.41 b

Results are expressed as mean values ± standard deviation (SD) and represent recovered compound amounts, calculated from concentrations in each fraction, corrected for fraction dry weight and normalized to the dry weight of the initial extruded sample. Data were analyzed by two-way ANOVA considering genotype and fraction (bioaccessible *vs.* non-bioaccessible), including their interaction, followed by Tukey–Kramer HSD *post hoc* test ($p < 0.05$). Different letters indicate statistically significant differences among genotype × fraction combinations. n.d., not detected.

starch and incompletely digested starch, which limits the attribution of potential fermentation-related effects exclusively to resistant starch.

Total phenolics recovered in the bioaccessible fraction ranged from 122 to 231 μmol per 100 g extrudate (dry weight basis), corresponding to 15–20% of the initial content. In contrast, 502–686 μmol per 100 g, representing 56–85%, remained in the non-bioaccessible fraction (Table 2). This limited release is consistent with previous reports in fiber-rich cereal matrices, where strong associations between phenolics and cell wall components restrict enzymatic hydrolysis. Microstructural evidence suggests that gastrointestinal digestion induces only minor alterations in fiber integrity, further limiting phenolic release.[17] Consequently, most phenolic compounds are expected to reach the colon largely intact, in agreement with previous findings.[14,16,17]

Regarding the phenolic profile, marked differences were observed between fractions, as shown in Table 2 and SI Table S2. Overall, flavan-3-ols were preferentially distributed in the bioaccessible fraction, averaging 56%, mainly due to their occurrence in free forms and their greater stability under gastrointestinal conditions.[40] Monomeric flavan-3-ols, such as catechin and epicatechin, predominated in the bioaccessible fraction, whereas dimeric and oligomeric forms, including procyanidins, were preferentially retained in the non-bioaccessible fraction. This pattern reflects underlying structural differences, as the lower molecular weight and higher solubility of monomeric compounds facilitate their release during digestion, whereas larger and more hydroxylated procyanidins exhibit reduced bioaccessibility due to stronger interactions with the matrix, in agreement with previous reports.[14]

Flavones were detected in both free and bound forms, although they were markedly more abundant in the free form. The bioaccessible fraction was dominated by methyl-luteolin-*O*-glucuronide and luteolin-7-*O*-glucuronide, particularly in DHL-151340 extrudate, whereas the non-bioaccessible fraction was characterized by methyl-luteolin (chrysoeriol). This contrasting distribution indicates that flavone bioaccessibility is strongly structure-dependent and is enhanced by conjugation with polar groups such as glucuronic acid, which increases hydrophilicity and solubility.[40,41]

Although total anthocyanins recovery in the purple-grain genotype DHL-151340 was low, these compounds were mainly found in the bioaccessible fraction, accounting for 63% of the total anthocyanins. This distribution is likely attributable to their polar and glycosylated structure, which favors solubilization under gastrointestinal digestion conditions.[40]

Phenolic acids were present in both free and bound forms, with the bound fraction predominating. Free phenolic acids were mainly recovered in the bioaccessible fraction, accounting for 67–100% of their total content, whereas bound phenolic acids were largely retained in the non-bioaccessible fraction, representing 62–92%. This distribution is consistent with their extensive esterification to cell wall polysaccharides, particularly arabinoxylans.[16,40]

Overall, the distribution of phenolic compounds between the bioaccessible and the non-bioaccessible fractions was mainly driven by structural features. Free and low-molecular-weight compounds were preferentially released during digestion, whereas cell wall-bound, polymeric, and more hydrophobic phenolics largely remained in the non-bioaccessible fraction and are therefore expected to reach the colon for further microbial transformation.

3.3. Fate of β-glucans and phenolic compounds during *in vitro* colonic fermentation

3.3.1. β-Glucan degradation and short-chain fatty acid production. A rapid and progressive decrease in β-glucan content was observed in all extruded genotypes during *in vitro* colonic fermentation, with most of the depletion occurring within the first 10 h of incubation (Fig. 1A). In all samples, β-glucans were almost completely depleted within 24–48 h, indicating their rapid utilization by the intestinal microbiota. This behavior is consistent with the high fermentability of cereal β-glucans previously reported for barley- and oat-based matrices.[14,42]

The progressive reduction in the β-glucan content during fermentation coincided with a marked increase in total SCFAs production in the extruded samples, particularly after 24 h. Fig. 1B–D show the main SCFAs, namely acetic, propionic, and butyric acids, whereas minor SCFAs, including isobutyric, isovaleric, valeric, and hexanoic acids, are reported in SI Table S3.

SCFAs were already detected at 0 h in all systems, reflecting basal microbial activity. However, as fermentation progressed, the SCFA profiles of the barley extrudates clearly diverged from the control. In all extruded samples, acetic acid increased rapidly during the early stages of fermentation, followed by a pronounced shift toward butyric production at later time points. By 48 h, butyric acid became the dominant SCFA in all extruded matrices, while propionic acid increased after 24 h but remained secondary. Branched-chain fatty acids and hexanoic acid showed moderate increases at late fermentation stages.

Among the extrudates, β-glucan-rich samples such as Hilose® and Annapurna® exhibited the highest butyric accumulation at 48 h, together with elevated acetic levels. This finding supports the role of barley β-glucans as readily fermentable substrates, that promot SCFAs formation, particularly butyric acid.[14]

Although a molar ratio close to 60 : 20 : 20 for acetic, propionic, and butyric acids, respectively, is often reported for dietary fiber fermentation, this distribution is strongly influenced by substrate characteristics and processing conditions.[43,44] In this context, the comparatively high proportion of butyric acid observed in the present study, accounting for approximately 36–43% of total SCFAs, suggests a fermentation pattern likely associated with extrusion-induced modifications of β-glucan structure.

In the control sample, SCFAs production was slower and mainly driven by acetic and propionic acids, with limited butyrate formation and relatively higher branched-chain fatty

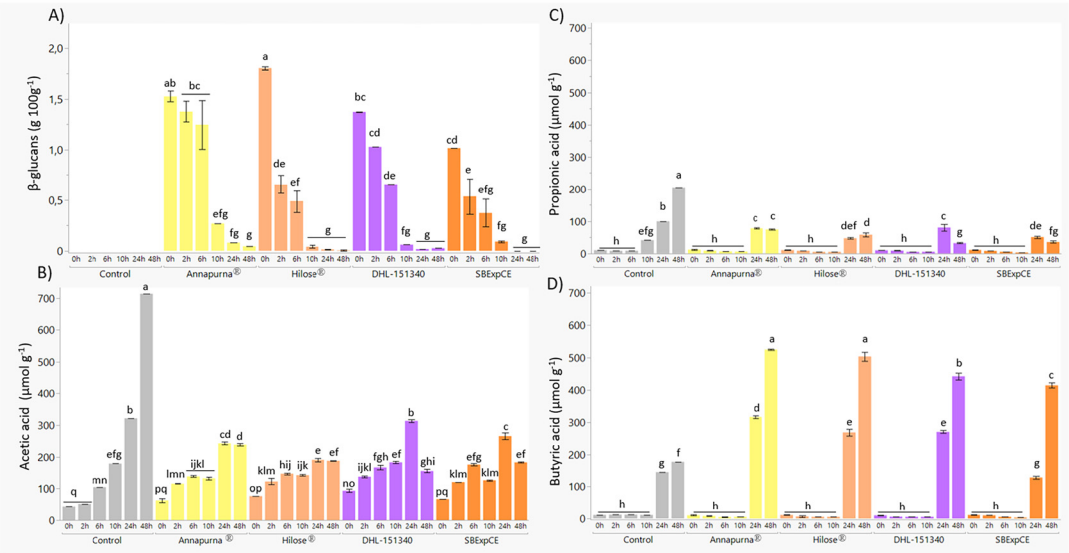

Fig. 1 β-Glucan content (g per 100 g) (A) and main short-chain fatty acids (SCFAs) (μmol g^{-1}): acetic acid (B), propionic acid (C), and butyric acid (D), measured at 0, 2, 6, 10, 24, and 48 h during *in vitro* colonic fermentation of the control and four barley extrudates (Annapurna®, Hilose®, DHL-151340, and SBExpCE). Data are shown as mean values. Two-way ANOVA showed significant effects of treatment, time, and their interaction ($p < 0.05$). Different letters indicate significant differences among treatment × time combinations according to Tukey–Kramer HSD *post hoc* test.

acids, indicating a greater contribution of proteolytic fermentation. In contrast, barley extrudates shifted fermentation towards a more butyrogenic profile as shown in Fig. 1B–D, and SI Table S3.

Taken together, these results indicate that the barley extrudates did not simply increase total fermentability, but promoted distinct fermentation outputs depending on matrix composition. In particular, the β-glucan-rich genotypes Hilose® and Annapurna® preferentially supported a more butyrogenic fermentation profile, highlighting their potential as substrates for the generation of SCFA-associated postbiotic responses.

3.3.2. Transformation of phenolic compounds and formation of derived phenolic metabolites. UPLC-MS/MS analysis allowed the identification and quantification of a total of 61 phenolic compounds, comprising 53 native phenolics (1 flavan-3-ols, 19 flavone glycosides, 8 anthocyanins, and 25 phenolic acids) and 8 microbial-derived metabolites (SI Table S4). Results obtained from the colonic fermentation assay showed overall comparable degradation kinetics of native phenolics and accumulation profiles of microbial metabolites across the four barley extrudates (Fig. 2). However, the purple extruded DHL-151340 exhibited slight differences in both phenolic degradation and the generation of new compounds, likely reflecting its higher overall phenolic content and the distinct phenolic profile.

Free flavone glycosides decreased rapidly in all samples within the first 2–6 h of fermentation (Fig. 2A). A similar trend was observed for anthocyanins in the purple-grain extrudate DHL-151340, which were no longer detectable after 10 h of fermentation (Fig. 2C). This behavior indicates rapid microbial utilization after release into the fermentation medium, consistent with an initial deglycosylation followed by further breakdown into smaller phenolic metabolites, as previously described under colonic conditions.[45] Bound flavone glycosides remained relatively stable in most genotypes (Fig. 2B), whereas a progressive decrease was observed in DHL-151340, suggesting increased susceptibility to microbial transformation at higher substrate availability in this genotype.

In contrast, free phenolic acids increased in all samples after 2 h of fermentation (Fig. 2D), while bound phenolic acids showed temporal fluctuations without a consistent decreasing trend (Fig. 2E). This pattern indicates a dynamic balance between the progressive release of ester-linked phenolics from the food matrix and their concurrent microbial transformation, rather than a simple transfer from the bound to the free pool.

Concomitantly, several low-molecular-weight phenolic metabolites progressively accumulated during fermentation (Fig. 2F), including 3-(4-hydroxy-3-methoxyphenyl)propanoic acid, hydroxyphenylacetic acids (4′-, 3′- and 2′-), hydroxyphenylpropanoic acid, phenylpropanoic acid, hydroxyphenylvaleric acid, and 3-(4-hydroxy-3,5-dimethoxyphenyl)propanoic acid (aka dihydrosinapic acid) (SI Table S4). Compared to the control, the extruded samples, particularly those derived from the purple-grain genotype DHL-151340, showed an earlier onset and more pronounced accumulation of these metabolites.

A clear temporal sequence of metabolite formation was observed during fermentation. The phenolic 3-(4-hydroxy-3-methoxyphenyl)propanoic acid increased at early stages (6–10 h), followed by the accumulation of hydroxyphenylacetic acids at intermediate time points, and subsequently by hydroxyphenylpropanoic acid at later stages (24–48 h). The latter exceeded 100 μmol per 100 g in several extrudates and emerged as a major end product of colonic polyphenol metabolism. This pattern suggests the occurrence of successive

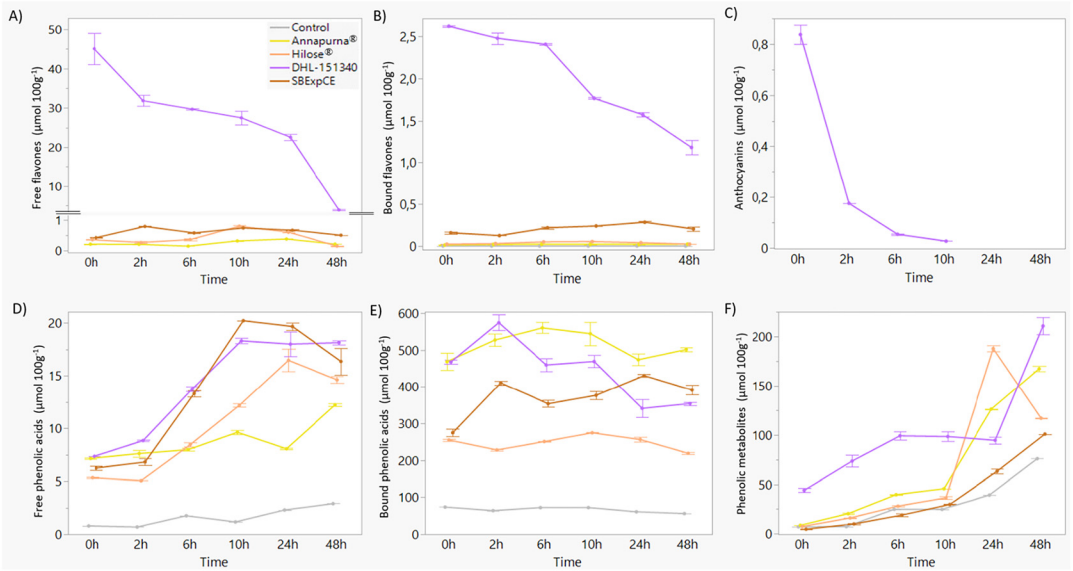

Fig. 2 Changes in native phenolic families and phenolic metabolites during *in vitro* colonic fermentation of the control and four barley extrudates (Annapurna®, Hilose®, DHL-151340, and SBExpCE). (A) Free flavone glycosides, (B) bound flavone glycosides, (C) anthocyanins, (D) free phenolic acids, (E) bound phenolic acids, and (F) total phenolic metabolites, expressed as µmol per 100 g, measured at 0, 2, 6, 10, 24, and 48 h of fermentation. Data are shown as mean ± SD.

microbial transformations of native phenolic compounds, involving reduction, dehydroxylation, and side-chain modifications. For instance, 4-hydroxy-3-methoxycinnamic acid derivatives may be converted into 3,4-dihydroxycinnamic acid-related intermediates, which are further transformed into hydroxyphenylacetic and hydroxyphenylpropanoic acids.[17]

In addition, hydroxybenzoic acid derivatives, including 4-hydroxybenzoic, 4-hydroxy-3-methoxybenzoic, and 3,4-dihydroxybenzoic acids, showed a tendency to increase at late fermentation stages (24–48 h) across all extruded samples (SI Table S4), in agreement with previous reports on colonic metabolism of cereal phenolics.[46,47] Taken together, these results support a coordinated microbial conversion of barley phenolic compounds into a limited number of low-molecular-weight metabolites. Based on these findings, a simplified metabolic pathway summarizing the main transformations of barley phenolics during colonic fermentation is proposed in Fig. 3. Overall, these findings indicate that barley phenolics were not merely degraded during fermentation, but underwent a structured microbial biotransformation process leading to a relatively defined set of low-molecular-weight catabolites. Importantly, the timing and relative abundance of these metabolites were influenced by the initial phenolic composition of the extruded matrix, supporting the idea that genotype-dependent differences remain functionally relevant even after extrusion and gastrointestinal digestion.

3.4. Effects of barley-based products on colonic microbiota composition

Microbiota profiling was used here not necessarily to identify completely distinct taxonomic endpoints for each barley genotype, but rather to determine whether the different extruded matrices generated divergent ecological trajectories or convergent fermentation-associated responses over time. This distinction is particularly relevant in *in vitro* batch systems, where temporal dynamics and substrate depletion often exert a stronger effect on microbial structure than subtle compositional differences between related cereal substrates.

As a first approach, changes in microbial diversity were evaluated using alpha and beta diversity metrics. All barley extrudates induced a significant decrease in observed ASVs compared to the control, although no major differences were observed among products (SI Fig. S2A). Shannon and Simpson indices also varied as a function of fermentation time and substrate, with a significant decrease in Shannon diversity observed for the DHL-151340 and SBExpCE extrudates. Such reductions in alpha diversity are commonly reported in batch fermentation systems supplemented with fermentable substrates, reflecting the selective enrichment of specialized microbial groups and a concomitant reduction in overall richness.[48] Beta diversity analysis revealed a clear modulation of the colonic microbiota driven by both substrate type and fermentation time. However, all barley treatments converged toward a similar microbial profile at 24 and 48 h (SI Fig. S2B), indicating that substrate availability and fermentation stage were the main drivers shaping microbial community structure and dynamics.

At the phylum level (SI Fig. S3), early fermentation stages (0–6 h) were characterized by an increase in Pseudomonadota and a concomitant decrease in Bacillota, Bacteroidota and Actinomycetota, particularly in response to some barley treatments. This pattern is typical of the initial phase of batch *in vitro* fermentations and reflects rapid ecological rearrange-

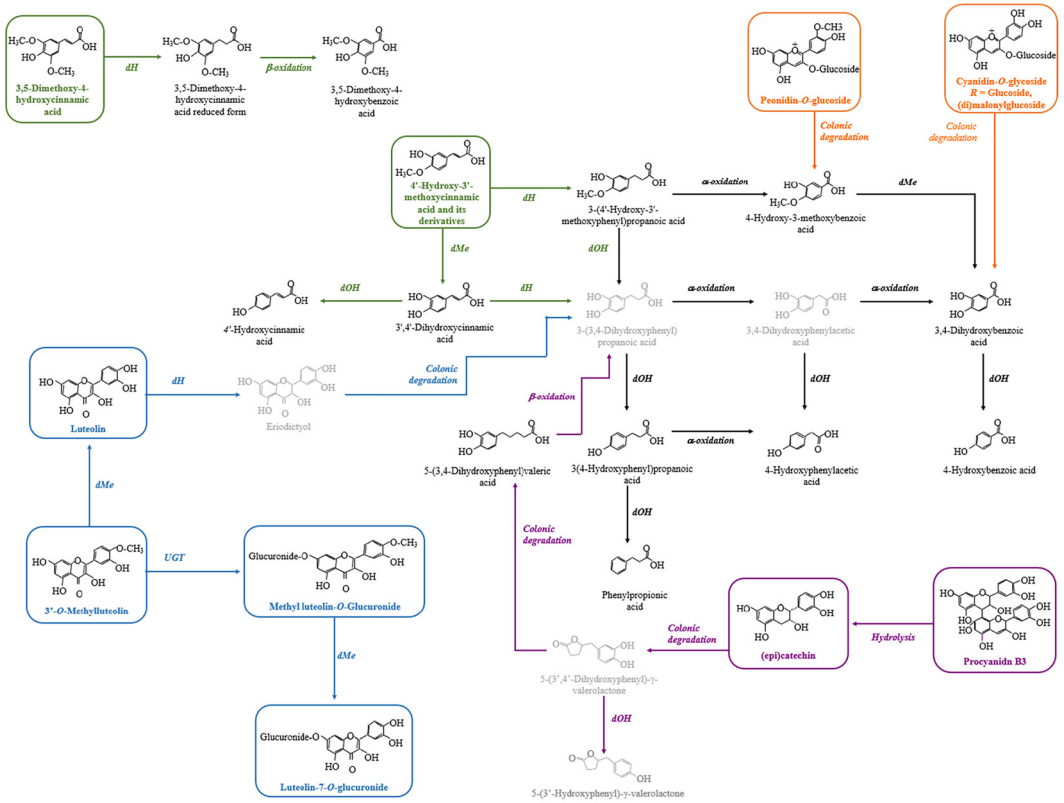

Fig. 3 Proposed metabolic pathways for microbial degradation of barley phenolics during colonic fermentation. Solid boxes indicate metabolites detected and quantified in the present study, whereas faded structures represent proposed intermediates. Major reactions include dOH (dehydroxylation), dH (dehydrogenation), dMe (demethylation), and side-chain shortening *via* α-oxidation and β-oxidation. Colors denote phenolic classes: flavan-3-ols (purple), flavones (blue), anthocyanins (orange), and phenolic acids (green).

ments driven by the availability of easily fermentable substrates.[48,49] Pseudomonadota, including fast-growing facultative anaerobes, can temporarily proliferate under these conditions. From 10 h onwards, a marked decrease in Pseudomonadota and a progressive enrichment in Bacillota were observed, particularly in response to the extrudates obtained from Annapurna® and Hilose®. This shift coincided with the accumulation of fermentation end-products and the establishment of more acidic and strictly anaerobic conditions, which favor obligate anaerobic and saccharolytic bacteria. Many of these bacteria belong to the Bacillota phylum and play a key role in polysaccharide degradation and butyrate production.[49]

At 24 and 48 h, all barley treatments showed a sustained decrease in Pseudomonadota and Bacteroidota and a dominance of Bacillota compared to the control, especially for the β-glucan-rich extrudates. These patterns are consistent with previous observations indicating that Pseudomonadota are less competitive under acidic, SCFA-rich conditions, whereas many Bacillota are better adapted to cross-feeding networks and the utilization of fermentation intermediates.[50] The decline in Bacteroidota at later stages likely reflects substrate depletion and competitive exclusion in non-renewed batch system.[42]

At the genus level (Fig. 4), analyses focused on time points from 6 h onwards, as earlier stages mainly reflect ecological adaptation rather than functionally stable fermentation.[48,51] At 6 h, all barley treatments promoted an increase in *Escherichia–Shigella* and *Streptococcus* and a decrease in genera such as *Bifidobacterium*, *Dialister* and *Gemmiger*, reflecting the transient predominance of fast-growing facultative anaerobes. At 10 h, treatment-specific responses became more evident; extruded products from Annapurna® and Hilose® showed a marked reduction in *Escherichia–Shigella*, whereas extruded SBExpCE and DHL-151340 promoted the co-occurrence of *Streptococcus* and *Megasphaera*. This pattern suggests the establishment of lactate-based cross-feeding interactions, which are characteristic of the transition toward a mature saccharolytic fermentation.[50,52]

At later fermentation stages (24–48 hours), an increase in commensal genera such as *Catenibacterium* was detected, consistent with advanced fermentation of complex carbohydrates. Concurrently, an enrichment of opportunistic taxa including *Klebsiella* and *Sutterella*, was observed. In the context of batch *in vitro* fermentation, such increases have been previously reported and are generally attributed to the absence of host-mediated regulatory mechanisms, including immune constraints and intestinal clearance, rather than necessarily indicating an adverse microbial shift.[51,52]

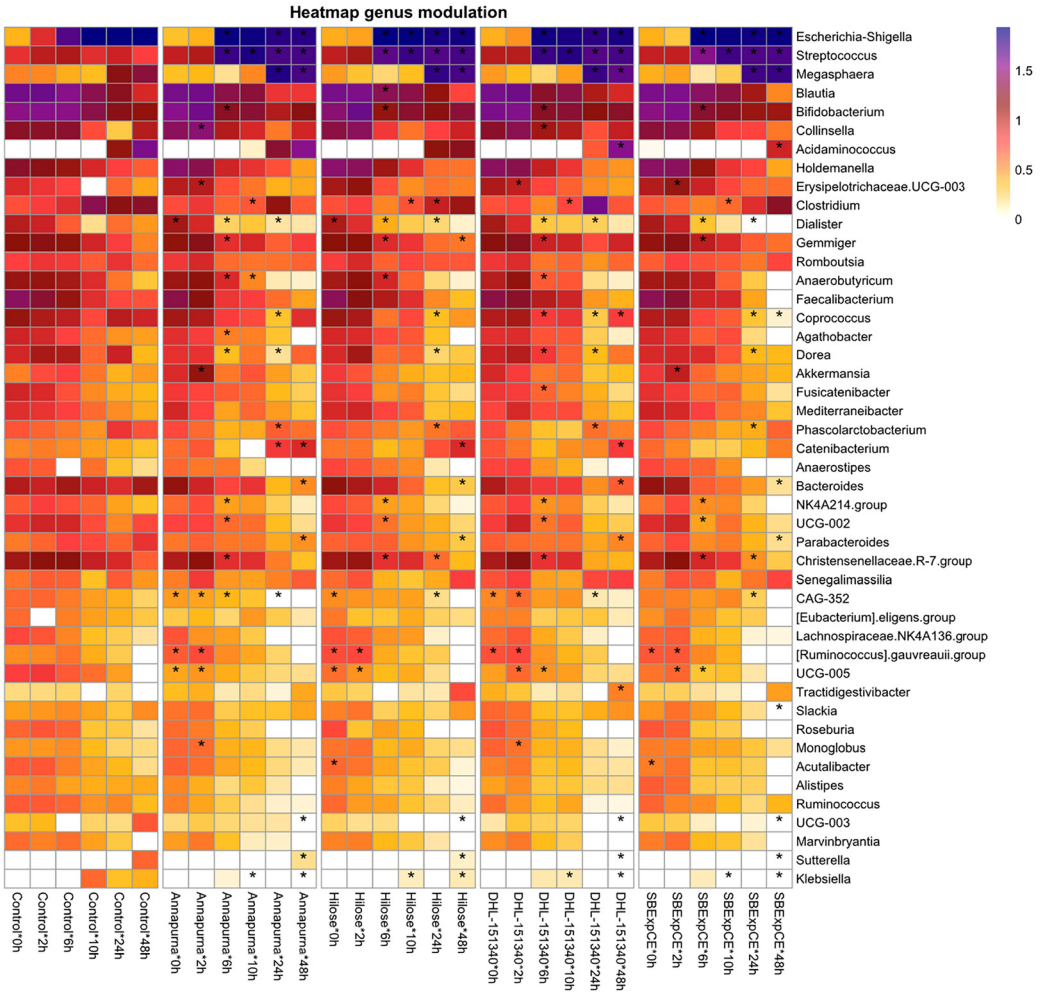

Fig. 4 Heatmap showing the evolution of relative abundance at the genus level according to barley extrudate and fermentation time. To improve data interpretation, values were normalized using square root transformation of log-transformed values: $\sqrt{(\log(x + 1))}$. Statistically significant differences were evaluated by two-way ANOVA followed by Games–Howell *post hoc* test. Asterisks indicate statistically significant differences ($p < 0.05$) compared to the digestion control (blank digestion without barley sample).

Across all barley treatments, a progressive decrease in *Bacteroides* and *Parabacteroides* was observed over time, likely reflecting substrate exhaustion, prolonged exposure to low pH, and competitive exclusion under non-renewed batch system. Similar declines in these genera during extended *in vitro* fermentations have been previously reported, particularly when complex polysaccharides become limiting.[42,48] Additionally, the extruded products derived from SBExpCE and DHL-151340 induced a reduction in *Acidaminococcus* and *Coprococcus*, which may be linked to a metabolic shift away from amino acid fermentation and to sensitivity to sustained acidic conditions.

Overall, the genus-level microbial changes reflected a typical *in vitro* fermentation succession, with early fast-growing taxa replaced by bacteria specialized in complex carbohydrate fermentation. This pattern suggests that the barley extrudates mainly influenced the timing and intensity of microbial succession rather than generating completely distinct community endpoints. Accordingly, the most informative differences among genotypes may lie less in final taxonomic composition than in the metabolic consequences of these shifts, particularly in relation to SCFAs production and phenolic catabolite generation.

It should be noted, however, that these microbial trajectories were obtained under static batch fermentation conditions, which do not fully reproduce the dynamic ecological environment of the human colon. In particular, the absence of pH control and continuous metabolite removal may progressively favor acid-tolerant and fast-growing taxa at later fermentation stages. Therefore, the microbial profiles observed at 24–48 h should be interpreted with caution and primarily as a comparative representation of substrate-driven responses under *in vitro* conditions, rather than as a direct reflection of *in vivo* colonic ecology.

Table 3 Significant positive Spearman correlations between major colonic microbial genera and native phenolic compounds, short-chain fatty acids (SCFAs), and microbial-derived phenolic metabolites during *in vitro* colonic fermentation of barley extrudates

	Acidaminococcus	*Megasphaera*	*Clostridium*	*Streptococcus*	*E. shigella*	*Phascolarotobacterium*	*Catenibacterium*	*Senegalimassila*
Native phenols								
OH benzoic acid	**	**		***				
B_syringic acid	**	***		***				
pOH benzoic acid	***	***		***	*			
Cinnamic acid				**	***			
B_VA		*		**				
B_OHBenzoic acid	*	*		*				
B_p.OHbenzoic acid	**	***	***					
B_p.coumaric acid				**				
B_m.coumaric acid				*				
Short-chain fatty acids								
Butyric	***	***	***			**	***	*
Propionic	***	***	***			**	***	*
Valeric	***	***	**					
Isovaleric	***	***	**				*	*
Acetic	***	***	**	*	***			
Hexanoic	***	***	**					
Isobutyric	**				***			
Metabolites								
OHPhProp acid	***	***	*	***	***			
DiHydroFA				***				
PhProp	***	**	**					
OHPhValeric acid		**						
o.OHPhAc acid	**				*			

Only positive correlations with $|r| \geq 0.7$ are shown. Significance levels are indicated as: * $p < 0.05$; ** $p < 0.01$; *** $p < 0.001$. Compounds with the prefix B-correspond to phenolic compounds from the bound fraction. OH benzoic acid: hydroxybenzoic acid; B_syringic acid: B_3,5-dimethoxy-4-hydroxybenzoic acid; pOH benzoic acid: 4-hydroxybenzoic acid, B_VA: B_4-hydroxy-3-methoxybenzoic acid; B_OHBenzoic acid: B_hydroxybenzoic acid; B_p.OHBenzoic acid: B_4-hydroxybenzoic acid; B_p.coumaric acid: B_4′-hydroxycinnamic acid (*cis*/*trans*); B_m.coumaric acid: B_3′-hydroxycinnamic acid (*cis*/*trans*); OHPhProp acid: hydroxyphenylpropanoic acid; DiHydroFA: 3-(4′-hydroxy-3′-methoxyphenyl)propanoic acid; PhProp: phenylpropanoic acid; OHPhValeric acid: hydroxyphenylvaleric acid; o.OHPhAc acid: 2′-hydroxyphenylacetic acid.

3.5. Associations between microbial taxa and metabolic outputs during colonic fermentation

To better understand the functional relationships underlying colonic fermentation, correlation analyses were performed integrating native bioactive compounds, SCFAs production, microbial composition, and microbial-derived phenolic metabolites. This approach was intended not only to identify co-occurrence patterns, but also to explore whether specific microbial taxa were consistently associated with the main metabolic outputs generated during fermentation. Significant positive associations are summarized in Table 3, whereas the full Spearman correlation matrices are provided in SI Fig. S4.

Strong positive correlations were observed between key fermentative genera, particularly *Megasphaera*, *Acidaminococcus*, and *Clostridium*-related taxa, and major SCFAs including acetic, propionic, butyric, and valeric acids (Table 3 and SI Fig. S4B). *Catenibacterium* also showed significant positive associations with butyric and propionic acids. These genera are commonly linked to saccharolytic fermentation, cross-feeding interactions, and late-stage anaerobic metabolism, supporting their functional relevance in the fermentative networks established in the present system.[53,54] Recent *in vitro* and *in vivo* studies have highlighted *Megasphaera* as a central lactate-utilizing taxon linking primary carbohydrate fermenters with downstream SCFAs production, while members of *Clostridium* and related *Firmicutes* remain major contributors to butyrate formation.[54,55] Conversely, *Escherichia–Shigella* and *Streptococcus* displayed comparatively fewer significant associations with SCFAs, being mainly linked to acetic acid (Table 3 and SI Fig. S4B), suggesting a more limited contribution to the broader SCFA profile characteristic of advanced saccharolytic fermentation. Similar inverse relationships between enteric or lactic acid bacteria and SCFAs accumulation have been reported in recent controlled fermentation models, where increasing SCFAs concentrations impose selective pressure on fast-growing facultative taxa.[43,56]

Several microbial-derived phenolic metabolites, particularly hydroxyphenylpropanoic acid and phenylpropanoic acid, were positively correlated with SCFA-associated genera, most notably *Acidaminococcus* and *Megasphaera*, and to a lesser extent *Clostridium*-related taxa (Table 3 and SI Fig. S4C). This co-occurrence suggests that phenolic biotransformation may overlap with microbial networks involved in active fermentation and SCFAs production. Recent evidence indicates that gut microbial conversion of dietary polyphenols into low-molecular-weight phenolic acids often relies on shared reductive and oxidative pathways within fermentative consortia.[57,58]

In contrast, several genera, such as *Coprococcus*, *Gemmiger*, *Dialister*, and *Bacteroides*, not positively associated with SCFAs or phenolic metabolites in SI Fig. S4, may represent microbial groups less involved in late-stage fermentative metabolism under these batch conditions.[57,59]

Native phenolic compounds, particularly hydroxybenzoic acid derivatives and several bound phenolic acids, also exhibited significant correlations with specific genera (Table 3 and SI Fig. S4A), indicating that parent phenolics may still contribute to shaping microbial associations during fermentation. This pattern aligns with recent metabolomic studies demonstrating that decreases in parent phenolic compounds during fermentation are typically accompanied by the emergence of smaller microbial-derived phenolic acids, reflecting active bioconversion processes.[19,20,57]

Overall, the correlation patterns indicate that SCFAs production and phenolic compound biotransformation are tightly interconnected processes occurring within a functionally mature fermentative microbiota. Genera positively associated with SCFAs were also linked to phenolic metabolite formation, supporting the concept of coordinated metabolic networks driven by cross-feeding and substrate specialization.[60] In contrast, taxa negatively correlated with both SCFAs and phenolic metabolites likely represent microbial groups disadvantaged under prolonged acidic and metabolite-rich conditions typical of batch *in vitro* fermentation. These findings underscore the value of correlation-based approaches for identifying functional microbial–metabolite relationships, while also highlighting the need for cautious interpretation given the host-free nature of *in vitro* systems.

4. Conclusions

This study demonstrates that extruded barley-based products retain relevant functional potential at the colonic level, despite processing-induced changes and the limited upper gastrointestinal bioaccessibility of many native phenolic compounds. A substantial proportion of β-glucans, digestion-resistant starch fractions, and phenolics remained in the non-bioaccessible fraction, supporting their role as substrates for microbial fermentation.

All extrudates promoted active colonic fermentation, characterized by SCFAs production, phenolic biotransformation, and time-dependent shifts in gut microbiota composition. Although microbial communities converged at later stages, distinct functional outputs were observed among genotypes. In particular, Annapurna® and Hilose® showed the strongest butyrogenic response, whereas DHL-151340 was distinguished by its phenolic profile and the formation of specific microbial-derived metabolites. Differences between genotypes with similar fibre and phenolic contents further suggest that matrix-related factors also contribute to fermentation behavior. Correlation analyses indicated that these functional outputs are driven by coordinated microbiota–metabolite interactions, linking SCFA-associated genera with both SCFAs production and phenolic catabolite formation.

Overall, the results highlight that the colonic fate of barley bioactives is shaped by both genotype and processing-induced matrix effects, leading to distinct fermentation and phenolic biotransformation footprints. These findings support the development of barley-based functional foods targeting gut microbial metabolism and warrant further validation using more physiologically relevant models and *in vivo* approaches.

Author contributions

Conceptualization: L. R.-P., M. M.; methodology: M. M. S., M. E. C. A., A. M., N. M., M. V. M.-A., I. F.; investigation: M. M. S., M. E. C. A.; formal analysis: M. M. S., M. E. C. A., A. M., L. R.-P. Data curation: M. M. S., M. E. C. A., N. M.; visualization: M. M. S., L. R.-P.; writing – original draft: M. M. S., M. E. C. A.; writing – review & editing: R. P., N. M., M. V. M.-A., M. M., L. R.-P.; resources: R. P., M. M., L. R.-P.; supervision: L. R.-P., M. M.; project administration: M. M., L. R.-P.; funding acquisition: L. R.-P., M. M.

Conflicts of interest

The authors declare that they have no known competing financial interests or personal relationships that could have appeared to influence the work reported in this paper.

Data availability

The datasets generated and analyzed during this study will be deposited in the CORA Research Data Repository (CSUC, https://dataverse.csuc.cat/) and made publicly available prior to publication. Additional supporting data are provided in the supplementary information (SI). Supplementary information is available. See DOI: https://doi.org/10.1039/d6fo00601a.

Acknowledgements

M. E. C. A. acknowledges the support of an AGAUR (2022 FI_B 00760) predoctoral fellowship. I. F. acknowledges the support of a predoctoral fellowship from Spanish Ministry of Science, Innovation, and Universities (PRE2021-100591). M. M. S. acknowledges the support of a postdoctoral contract from the University of Lleida. This work was supported by the competitive project BARGUT (ref. P16079), entitled "Impact of new barley genotypes biofortified in bioactive compounds on the gut microbiome and metabolome", funded by the Fundació Centre de Recerca en Agrotecnologia (Agrotecnio), Lleida, Spain.

References

1 A. Kaur, S. S. Purewal, Y. Phimolsiripol, *et al.*, Unraveling the hidden potential of barley (*Hordeum vulgare*): An important review, *Plants*, 2024, **13**, 2421, DOI: 10.3390/plants13172421.
2 M. Blandino, M. Locatelli, V. Sovrani, *et al.*, Progressive pearling of barley kernel: Chemical characterization of pearling fractions and effect of their inclusion on the nutritional and technological properties of wheat bread, *J. Agric. Food Chem.*, 2015, **63**, 5875–5884, DOI: 10.1021/jf506193p.
3 P. Sharma and H. S. Gujral, Cookie making behavior of wheat–barley flour blends and effects on antioxidant properties, *LWT – Food Sci. Technol.*, 2014, **55**, 301–307, DOI: 10.1016/j.lwt.2013.08.019.
4 E. Idehen, Y. Tang and S. Sang, Bioactive phytochemicals in barley, *J. Food Drug Anal.*, 2017, **25**, 148–161, DOI: 10.1016/j.jfda.2016.08.002.
5 P. de Graaff, C. Govers, H. J. Wichers, *et al.*, Consumption of β-glucans to spice up T cell treatment of tumors: a review, *Expert Opin. Biol. Ther.*, 2018, **18**, 1023–1040, DOI: 10.1080/14712598.2018.1523392.
6 EFSA, Scientific Opinion on the substantiation of health claims related to beta-glucans from oats and barley and maintenance of normal blood LDL-cholesterol concentrations (ID 1236, 1299), increase in satiety leading to a reduction in energy intake (ID 851, 852), *EFSA J.*, 2011, **9**, 2207, DOI: 10.2903/j.efsa.2011.2207.
7 C. McCarthy, E. Papada and A. Z. Kalea, The effects of cereal β-glucans on cardiovascular risk factors and the role of the gut microbiome, *Crit. Rev. Food Sci. Nutr.*, 2025, **65**, 2489–2505, DOI: 10.1080/10408398.2024.2345159.
8 X. Wang, C. Peng, J. Fan, *et al.*, Comparative analysis of β-glucan, phenolic compounds, and targeted metabolomics in whole-grain highland barley varieties: Effects of cooking-induced changes, *Food Chem.: X*, 2025, **29**, 102675, DOI: 10.1016/j.fochx.2025.102675.
9 X. Xiao, J. Li, H. Xiong, *et al.*, Effect of extrusion or fermentation on physicochemical and digestive properties of barley powder, *Front. Nutr.*, 2022, **8**, 794355, DOI: 10.3389/fnut.2021.794355.
10 F. Ge, Y. Sun, C. Yang, *et al.*, Exploring the relationship between starch structure and physicochemical properties: The impact of extrusion on highland barley flour, *Food Res. Int.*, 2024, **183**, 114226, DOI: 10.1016/j.foodres.2024.114226.
11 I. Friero, M. Martínez-Subirà, A. Macià, *et al.*, Exploring the nutritional and techno-functional benefits of purple hull-less barley in extruded ready-to-eat cereals, *LWT – Food Sci. Technol.*, 2024, **212**, 117018, DOI: 10.1016/j.lwt.2024.117018.
12 A. S. Hole, N. P. Kjos, S. Grimmer, *et al.*, Extrusion of barley and oat improves the bioaccessibility of dietary phenolic acids in growing pigs, *J. Agric. Food Chem.*, 2013, **61**, 2739–2747, DOI: 10.1021/jf3045236.
13 J. Bindelle, R. Pieper, C. A. Montoya, *et al.*, Nonstarch polysaccharide-degrading enzymes alter the microbial community and fermentation patterns, *FEMS Microbiol. Ecol.*, 2011, **76**, 553–563, DOI: 10.1111/j.1574-6941.2011.01074.x.
14 J. I. Mosele, M.-J. Motilva and I. A. Ludwig, Beta-glucan and phenolic compounds: Their concentration and behavior during digestion and fermentation, *J. Agric. Food Chem.*, 2018, **66**, 8966–8975, DOI: 10.1021/acs.jafc.8b02240.
15 C. Martin-Gallausiaux, L. Marinelli, H. M. Blottière, *et al.*, SCFA: mechanisms and functional importance in the gut, *Proc. Nutr. Soc.*, 2021, **80**, 37–49, DOI: 10.1017/S0029665120006916.

16 S. Zheng, H. Zhang, R. Liu, *et al.*, Do short chain fatty acids and phenolic metabolites have synergistic anti-inflammatory effects? – New insights from a TNF-α-induced Caco-2 cell model, *Food Res. Int.*, 2021, **139**, 109833, DOI: 10.1016/j.foodres.2020.109833.
17 Y. Zhao, F. Leng, S. Fan, *et al.*, Changes of barley bound phenolics during digestion and fermentation, *Foods*, 2025, **14**, 1114, DOI: 10.3390/foods14071114.
18 C. Cueva, I. Gil-Sánchez, B. Ayuda-Durán, *et al.*, Effects of wine polyphenols on gut and host health, *Molecules*, 2017, **22**, 99, DOI: 10.3390/molecules22010099.
19 J. C. Espín, A. González-Sarrías and F. A. Tomás-Barberán, The gut microbiota: A key factor in therapeutic effects of polyphenols, *Biochem. Pharmacol.*, 2017, **139**, 82–93, DOI: 10.1016/j.bcp.2017.04.033.
20 I. Fernandez-Jalao, M. de las, N. Siles-Sánchez, S. Santoyo, *et al.*, Modulation of gut microbiota composition and microbial phenolic catabolism of phenolic compounds from *Achillea millefolium* L. and *Origanum majorana* L., *J. Agric. Food Chem.*, 2025, **73**, 478–494, DOI: 10.1021/acs.jafc.4c07910.
21 R. Yang, L. Gong, Y. Li, *et al.*, Role of the gut microbiota in determining the metabolic fate of free and bound phenolic compounds in wheat bran, *LWT – Food Sci. Technol.*, 2024, **210**, 116892, DOI: 10.1016/j.lwt.2024.116892.
22 S. Ntouranidi, C. Fryganas, V. Fogliano, *et al.*, In vitro utilization of barley husk by human gut microbiota depends on husk composition and particle size, *Food Res. Int.*, 2025, **221**, 117136, DOI: 10.1016/j.foodres.2025.117136.
23 C. D. Kay, M. N. Clifford, P. Mena, *et al.*, Recommendations for standardizing nomenclature for dietary (poly)phenol catabolites, *Am. J. Clin. Nutr.*, 2020, **112**, 1051–1068, DOI: 10.1093/ajcn/nqaa204.
24 C. Curti, M. N. Clifford, C. D. Kay, *et al.*, Extended recommendations on the nomenclature for microbial catabolites of dietary (poly)phenols, with a focus on isomers, *Food Funct.*, 2025, **16**, 3963–4000, DOI: 10.1039/D4FO06152G.
25 A. Brodkorb, L. Egger, M. Alminger, *et al.*, INFOGEST static in vitro simulation of gastrointestinal food digestion, *Nat. Protoc.*, 2019, **14**, 991–1014, DOI: 10.1038/s41596-018-0119-1.
26 S. Pérez-Burillo, S. Molino, B. Navajas-Porras, *et al.*, An in vitro batch fermentation protocol for studying the contribution of food to gut microbiota composition and functionality, *Nat. Protoc.*, 2021, **16**, 3186–3209, DOI: 10.1038/s41596-021-00537-x.
27 M.-E. Cortijo-Alfonso, S. Yuste, I. Friero, *et al.*, Metabolic profiling of (poly)phenolic compounds in mouse urine following consumption of hull-less and purple-grain barley, *Food Funct.*, 2024, **15**, 8300–8309, DOI: 10.1039/D4FO01275E.
28 L. Calderón-Pérez, M. J. Gosalbes, S. Yuste, *et al.*, Gut metagenomic and short chain fatty acids signature in hypertension: a cross-sectional study, *Sci. Rep.*, 2020, **10**, 6436, DOI: 10.1038/s41598-020-63475-w.
29 B. J. Callahan, P. J. McMurdie, M. J. Rosen, *et al.*, DADA2: High-resolution sample inference from Illumina amplicon data, *Nat. Methods*, 2016, **13**, 581–583, DOI: 10.1038/nmeth.3869.
30 I. Friero, A. Macià, M.-P. Romero, *et al.*, Unlocking phenolic potential: Determining the optimal grain development stage in hull-less barley genotypes with varying grain color, *Foods*, 2024, **13**, 1841, DOI: 10.3390/foods13121841.
31 G. Goudar, P. Sharma, S. Janghu, *et al.*, Effect of processing on barley β-glucan content, its molecular weight and extractability, *Int. J. Biol. Macromol.*, 2020, **162**, 1204–1216, DOI: 10.1016/j.ijbiomac.2020.06.208.
32 C. Roye, M. Henrion, H. Chanvrier, *et al.*, Extrusion-cooking modifies physicochemical and nutrition-related properties of wheat bran, *Foods*, 2020, **9**, 738, DOI: 10.3390/foods9060738.
33 Y. Zhao, X. Dang, H. Du, *et al.*, Understanding the impact of extrusion treatment on cereals: Insights from alterations in starch physicochemical properties and in vitro digestion kinetics, *Animals*, 2024, **14**, 3144, DOI: 10.3390/ani14213144.
34 S. A. Wani and P. Kumar, Effect of extrusion on the nutritional, antioxidant and microstructural characteristics of nutritionally enriched snacks, *J. Food Process. Preserv.*, 2016, **40**, 166–173, DOI: 10.1111/jfpp.12593.
35 R. J. Espinoza-Moreno, C. Reyes-Moreno, J. Milán-Carrillo, *et al.*, Healthy ready-to-eat expanded snack with high nutritional and antioxidant value produced from whole amarantin transgenic maize and black common bean, *Plant Foods Hum. Nutr.*, 2016, **71**, 218–224, DOI: 10.1007/s11130-016-0551-8.
36 S. M. Tosh, Review of human studies investigating the postprandial blood-glucose lowering ability of oat and barley food products, *Eur. J. Clin. Nutr.*, 2013, **67**, 310–317, DOI: 10.1038/ejcn.2013.25.
37 N. Mäkelä, O. Brinck and T. Sontag-Strohm, Viscosity of β-glucan from oat products at the intestinal phase of the gastrointestinal model, *Food Hydrocolloids*, 2020, **100**, 105422, DOI: 10.1016/j.foodhyd.2019.105422.
38 Z. Zhang, M. Zhu, B. Xing, *et al.*, Effects of extrusion on structural properties, physicochemical properties and in vitro starch digestibility of Tartary buckwheat flour, *Food Hydrocolloids*, 2023, **135**, 108197, DOI: 10.1016/j.foodhyd.2022.108197.
39 R. Dávila León, M. González-Vázquez, K. E. Lima-Villegas, *et al.*, In vitro gastrointestinal digestion methods of carbohydrate-rich foods, *Food Sci. Nutr.*, 2024, **12**, 722–733, DOI: 10.1002/fsn3.3841.
40 B. Ed Nignpense, N. Francis, C. Blanchard, *et al.*, Bioaccessibility and bioactivity of cereal polyphenols: A review, *Foods*, 2021, **10**, 1595, DOI: 10.3390/foods10071595.
41 L. Hu, Y. Luo, J. Yang, *et al.*, Botanical flavonoids: Efficacy, absorption, metabolism and advanced pharmaceutical technology for improving bioavailability, *Molecules*, 2025, **30**, 1184, DOI: 10.3390/molecules30051184.
42 S. A. Hughes, P. R. Shewry, G. R. Gibson, *et al.*, In vitro fermentation of oat and barley derived β-glucans by human

faecal microbiota, *FEMS Microbiol. Ecol.*, 2008, **64**, 482–493, DOI: 10.1111/j.1574-6941.2008.00478.x.

43 G. den Besten, K. van Eunen, A. K. Groen, *et al.*, The role of short-chain fatty acids in the interplay between diet, gut microbiota, and host energy metabolism, *J. Lipid Res.*, 2013, **54**, 2325–2340, DOI: 10.1194/jlr.R036012.

44 T. Immerstrand, K. E. Andersson, C. Wange, *et al.*, Effects of oat bran, processed to different molecular weights of β-glucan, on plasma lipids and caecal formation of SCFA in mice, *Br. J. Nutr.*, 2010, **104**, 364–373, DOI: 10.1017/S0007114510000553.

45 M. Domínguez-Fernández, I. A. Ludwig, M.-P. De Peña, *et al.*, Bioaccessibility of Tudela artichoke (Cynara scolymus cv. Blanca de Tudela) (poly)phenols: The effects of heat treatment, simulated gastrointestinal digestion and human colonic microbiota, *Food Funct.*, 2021, **12**, 1996–2011, DOI: 10.1039/D0FO03119D.

46 L. Zhang, T. Wu, Y. Zhang, *et al.*, Release of bound polyphenols from wheat bran soluble dietary fiber during simulated gastrointestinal digestion and colonic fermentation in vitro, *Food Chem.*, 2023, **402**, 134111, DOI: 10.1016/j.foodchem.2022.134111.

47 Y. Zhang, Y. Li, X. Ren, *et al.*, The positive correlation of antioxidant activity and prebiotic effect about oat phenolic compounds, *Food Chem.*, 2023, **402**, 134231, DOI: 10.1016/j.foodchem.2022.134231.

48 T. Gnanasekaran, J. Assis Geraldo, D. W. Ahrenkiel, *et al.*, Ecological adaptation and succession of human fecal microbial communities in an automated in vitro fermentation system, *mSystems*, 2021, **6**, e0023221, DOI: 10.1128/msystems.00232-21.

49 X. Wang, G. R. Gibson, A. Costabile, *et al.*, Prebiotic supplementation of in vitro fecal fermentations inhibits proteolysis by gut bacteria, and host diet shapes gut bacterial metabolism and response to intervention, *Appl. Environ. Microbiol.*, 2019, **85**, e02749-18, DOI: 10.1128/AEM.02749-18.

50 F. Moens, M. Verce and L. De Vuyst, Lactate- and acetate-based cross-feeding interactions between selected strains of lactobacilli, bifidobacteria and colon bacteria in the presence of inulin-type fructans, *Int. J. Food Microbiol.*, 2017, **241**, 225–236, DOI: 10.1016/j.ijfoodmicro.2016.10.019.

51 T. Van de Wiele, P. Van den Abbeele and W. Ossieur, *et al.*, *The simulator of the human intestinal microbial ecosystem (SHIME®)*, in *The Impact of Food Bioactives on Health*, Springer International Publishing, Cham, 2015, pp. 305–317, DOI: 10.1007/978-3-319-16104-4_27.

52 S. Fehlbaum, C. Chassard, M. C. Haug, *et al.*, Design and investigation of PolyFermS in vitro continuous fermentation models inoculated with immobilized fecal microbiota mimicking the elderly colon, *PLoS One*, 2015, **10**, e0142793, DOI: 10.1371/journal.pone.0142793.

53 P. Louis and H. J. Flint, Formation of propionate and butyrate by the human colonic microbiota, *Environ. Microbiol.*, 2017, **19**, 29–41, DOI: 10.1111/1462-2920.13589.

54 S. Zhao, R. Lau, Y. Zhong, *et al.*, Lactate cross-feeding between Bifidobacterium species and Megasphaera indica contributes to butyrate formation in the human colonic environment, *Appl. Environ. Microbiol.*, 2024, **90**, e0101923, DOI: 10.1128/aem.01019-23.

55 M. Vital, A. C. Howe and J. M. Tiedje, Revealing the bacterial butyrate synthesis pathways by analyzing (meta) genomic data, *mBio*, 2014, **5**, e00889, DOI: 10.1128/mBio.00889-14.

56 P. Sankarganesh, A. Bhunia, A. Ganesh Kumar, *et al.*, Short-chain fatty acids (SCFAs) in gut health: Implications for drug metabolism and therapeutics, *Med. Microecol.*, 2025, **25**, 100139, DOI: 10.1016/j.medmic.2025.100139.

57 I. Rowland, G. Gibson, A. Heinken, *et al.*, Gut microbiota functions: Metabolism of nutrients and other food components, *Eur. J. Nutr.*, 2018, **57**, 1–24, DOI: 10.1007/s00394-017-1445-8.

58 A. Duda-Chodak, T. Tarko, P. Satora, *et al.*, Interaction of dietary compounds, especially polyphenols, with the intestinal microbiota: A review, *Eur. J. Nutr.*, 2015, **54**, 325–341, DOI: 10.1007/s00394-015-0852-y.

59 F. Cardona, C. Andrés-Lacueva, S. Tulipani, *et al.*, Benefits of polyphenols on gut microbiota and implications in human health, *J. Nutr. Biochem.*, 2013, **24**, 1415–1422, DOI: 10.1016/j.jnutbio.2013.05.001.

60 E. J. Culp and A. L. Goodman, Cross-feeding in the gut microbiome: Ecology and mechanisms, *Cell Host Microbe*, 2023, **31**, 485–499, DOI: 10.1016/j.chom.2023.03.016.